Proceedings of The National Conference
On Undergraduate Research (NCUR) 2016
University of North Carolina Asheville
Asheville, North Carolina
April 7-9, 2016

Studying the Connection Between X-ray and UV Outflows in PG 1126-041

Zane Comden[1] Michael Gibbons[1] C.M. April[1] Margherita Giustini[2]
[1]Department of Physics and Astronomy
Humboldt State University
Arcata, California 95521 USA

[2]SRON - Netherlands Institute for Space Research
York University
University of Toronto

Faculty Advisor: Dr. Paola Rodriguez Hidalgo[1]

Abstract

Active Galactic Nuclei are still somewhat of an enigma; young, bright galaxies with a large range of redshifts. The high luminosity characteristics of the active galactic nucleus are attributable to accretion of gas and dust into a supermassive black hole at the center of the galaxy. The current research of this team is focused on gas outflows from the active galactic nucleus (AGN). These outflows are identified by broad absorption lines in the spectra of AGN. Current multi-epoch observations of many active galactic nuclei (AGN) have resulted in broad absorption lines that appear and disappear over time. Current observations show that these outflows have speeds up to 0.2c. The ultimate goal of this team is to understand the mechanism that drives quasar outflows and characterize the broad spectral absorption lines, as well as why the outflows are variable. This paper presents a study on PG 1126-041, a Seyfert galaxy with an active nucleus for which data has been obtained through Hubble Space Telescope (HST) and X-ray Multi-Mirror-Newton (XMM). PG 1126-041 is a low redshift (z=0.06), luminous Seyfert galaxy which displays very variable X-ray absorption. The data show results of the variability study of coordinated X-ray and UV-optical observations of PG 1126-041 (using data from XMM and HST respectively), searching for possible trends between variable X-ray absorption from the AGN, and the outflows characterized by variable broad absorption lines that this group are attempting to study.

Keywords: X-ray, Outflows, Active Galactic Nuclei

1. Introduction

Active Galactic Nuclei (AGN) are compact regions at the center of galaxies that exhibit extremely high luminosity. This luminosity of active nuclei is primarily powered by accretion onto a super massive black hole at the center of the galactic nucleus [1]. In the last 15 years, astronomers have found over one hundred thousand AGN, over ten times as many found before the year 2000[2]. Over the past decade there has been an increase in enthusiasm for studying AGN, which, paired with advances in astronomy technology has allowed astronomers to find more AGN than ever before. Despite this increase in interest, much is still unknown about the structure and mechanisms of AGN.

This team's work focuses on what are known as AGN outflows. Outflows are large quantities of gas, dust, and ions that are ejected from the AGN at up to relativistic speeds. These outflows are characterized by absorption lines in the spectrum of the AGN. Absorption lines are created by ejected material absorbing light emitted by the active nucleus and being ionized, and appear as troughs in the spectrum of the AGN. Absorption lines can be narrow, known as

narrow absorption lines (NALs), or broad, known as broad absorption lines (BALs). The velocities of these outflows are determined by the relative blue-shift of the absorption lines compared to their rest-frame wavelengths. Multiple absorption lines can be found throughout the spectrum of a single AGN[3]

These outflows have been shown to be variable over time[4]. The reason for this variability is still unknown, but several hypotheses have been put forward to explain this variability, including changes in the levels of ionization, or motions of absorbing clouds along the line of sight[5].

Due to the high luminosity of AGN coupled with their very small angular resolution, not much is known about structure of AGN and the driving forces behind these outflows. By gaining a better understanding of the relationship between variability of absorption in the X-ray range of wavelengths compared to variability of absorption lines in the UV, this team hopes to better understand the mechanics driving these outflows. According to current theoretical models of AGN structure, outflows cannot simply be driven by radiation pressure of the AGN. Radiation pressure capable of ejecting these outflows at such high speeds would exceed what is known as the Eddington limit, a maximum limit on the luminosity of an AGN in relation to the mass of its central black hole. An AGN with luminosity exceeding the Eddington limit would have a greater force of radially outward radiation pressure than radially inward gravitational forces, and the gas will be blown away from the nucleus by radiation pressure[6].

PG 1126-041 (also known as Mrk 1298) was chosen for this case study for several reasons. Firstly, it is known that the AGN is variable in its X-ray absorption [5]. Secondly, it is difficult to detect X-ray emissions from high-redshift AGN, especially when the X-ray emissions are relatively low, so studies such as this one are only attainable with low redshift AGN such as PG1126-041 (z=0.061).

This paper presents results of spectra taken with Hubble Space Telescope (HST) close in time to the X-ray observations captured by XMM-Newton and show a relationship between the X-ray and UV absorption levels over time.

2. Methods/Data

2.1 Observations with XXM-Newton

Three observations were taken with X-ray Multi-Mirror Mission (XMM-Newton) observatory in the month of June 2014. These observations gave absorption variability with which to compare our UV observation data. The XMM-Newton observations were taken within at most two days of the scheduled HST observations. The data from the observations is presented below, with less absorption in the second epoch (red) than in the first and third epochs (black and green respectively)(Figure 1**)**.

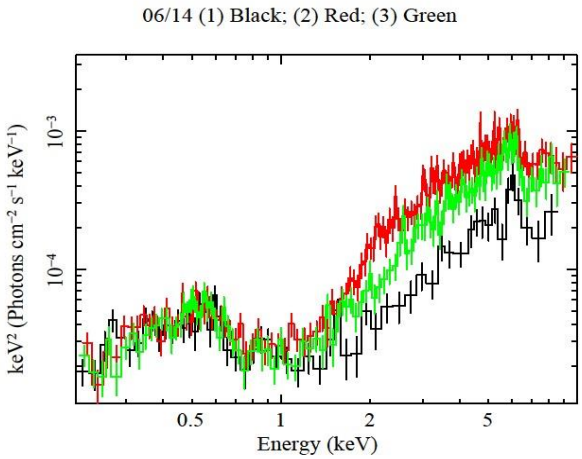

Figure 1: Three epochs of XMM-Newton observations overlaid. Epoch 1, June 1, 2014 (Black), epoch 2, June 12, 2014 (Red), and epoch 3, June 28, 2014 (Green)

2.2 Observations with HST

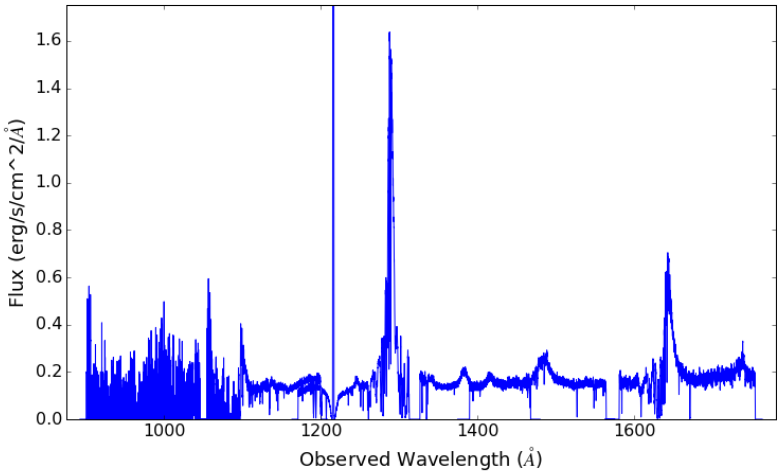

Figure 2: Full HST spectrum of PG 1126-041, June 1, 2014. The vertical line at approximately 1200 Å is an error caused by a malfunctioning pixel in the sensor.

Three different epochs of Hubble observations close in time to the X-ray observations made by XMM-Newton at three different times in the month of June 2014 (June 1, June 12, June 28) were used to study the relation between the X-ray and UV absorption. Two different gratings (G130M, G160M) were used for the Hubble observations to get the range of wavelengths required for our analysis. The first epoch spectrum taken with these gratings is shown in Figure 2. Gratings were selected that include the known absorption transitions Oxygen VI (Oxygen five times ionized, OVI), Phosphorous V (Phosphorous four times ionized, PV), Nitrogen V (Nitrogen four times ionized, NV), Silicon IV (Silicon three times ionized, SiIV), Carbon IV (Carbon three times ionized, CIV), as well as the Lyman-alpha transition.

Table 1: A table of the rest-frame ion transition wavelengths of investigation. These wavelengths were used to calculate locations of absorption in the spectrum of PG1126-041. The Lyman-alpha transition does not have a secondary absorption line.

Absorption Transition	Primary Absorption Rest-Frame Wavelength	Secondary Absorption Rest-Frame Wavelength
OVI	1031 Å	1037 Å
PV	1118 Å	1128 Å
NV	1238 Å	1242 Å
SiIV	1393 Å	1402 Å
CIV	1548 Å	1551 Å
Lyman-alpha	1216 Å	--------

The elemental transitions other than the Lyman series are known as doublets, meaning that two absorption lines are present in the spectrum at the rest-frame values listed in Table 1. The longer wavelength absorption line is shallower than the primary, shorter wavelength absorption line. Using a Python script to extract the Hubble data from the Flexible Image Transport System (FITS) files, spectra were plotted and transition line absorptions were compared among the 3 different epochs. Data was normalized by fitting a line to the continuum of the spectrum and correcting for differences in the slope of this line between the three epochs. A constant was added to every flux value in the data so the continuum line is horizontal at 1.00 on the vertical axis. This line is represented in Figures 3-8 by a horizontal dashed line. The data was then re-scaled for readability on the vertical axis. Areas where the gratings overlapped were combined using an average of the flux values, weighted by their respective error values. In the plots for PV and SiIV (Figures 3 and 4, respectively) this data manipulation is visible by a shift in the continuum of the spectrum at approximately 1170 Å and 1200 Å (Figure 3), as well as 1467 Å (Figure 4).

Six different redshift values were calculated by inspection of the CIV BALs using the redshift calculation formula

$$z_{abs} = \frac{\lambda_0 - \lambda_e}{\lambda_e}, \quad (1)$$

where the value of z_{abs} is the absorption redshift value calculated from λ_0, the observed absorption wavelength of CIV and λ_e, the rest-frame absorption wavelength of CIV. After calculating these z_{abs} redshift values with equation (1), the rest-frame wavelengths of the different transitions listed in Table 1 were used as λ_e to obtain the absorption wavelength:

$$\lambda_0 = (z_{abs} + 1)\lambda_e. \quad (2)$$

The resulting λ_0 are the corresponding absorption lines and their doublet pairs indicated by vertical lines in Figures 3-8. The primary transition wavelengths are indicated with black dashed lines and their doublet pairs are indicated with red, finely dotted lines.

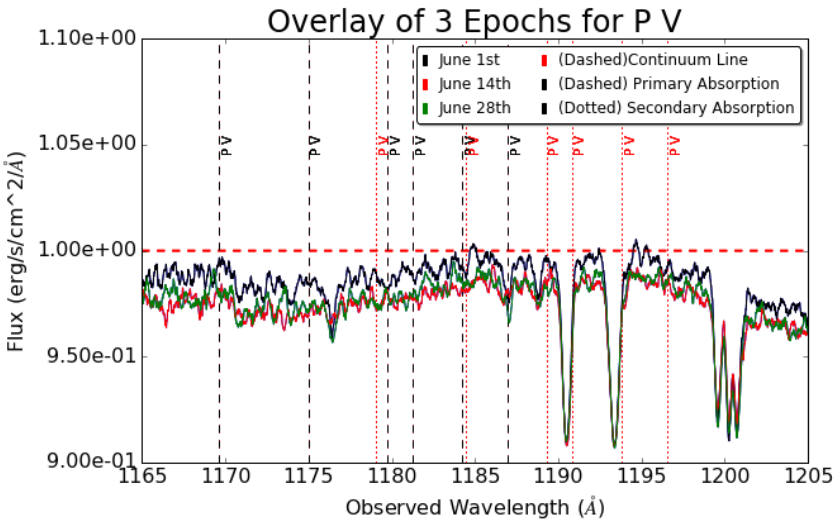

Figure 3: Overlay of 3 epochs of observation for Phosphorous V BALs. Unlike the X-ray measurements, the average level of absorption is lower in the first epoch than in the second and third epochs. There is an absorption line at approximately 1176 Å in the first and third epochs that is not present in the second epoch.

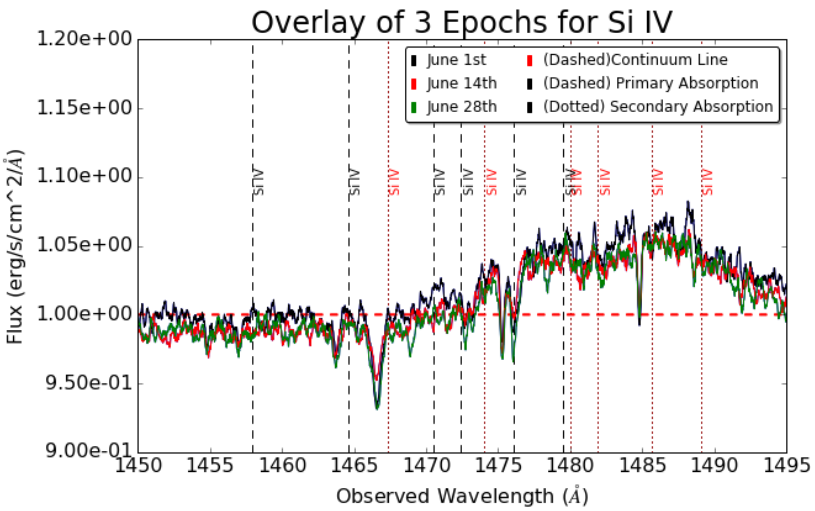

Figure 4: Overlay of three epochs of observation for Silicon IV BALs. The absorption at ~1466.5 Å is significantly lower in the second epoch than the first and third epochs.

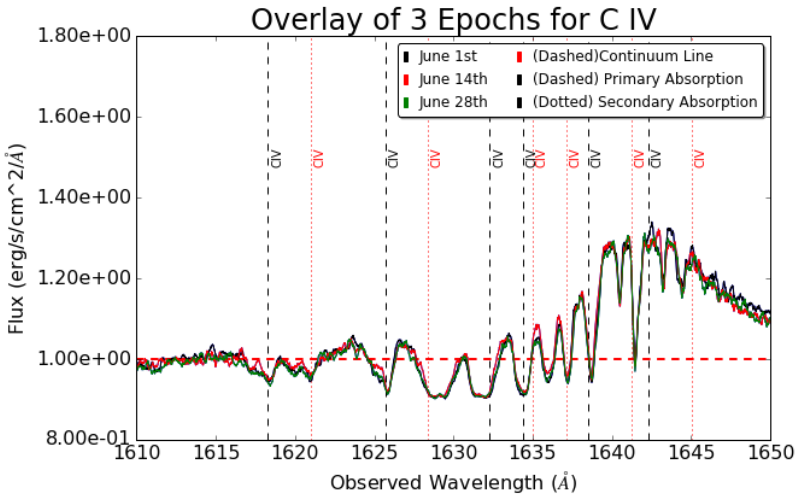

Figure 5: Overlay of all three epoch observations for Carbon IV BALs. The absorption locations indicated in this plot were extrapolated to the other regions of investigation using equations 1 and 2. From ~1630 Å to ~1638 Å the level of absorption in the second epoch is noticeably lower than the absorption in the first and third epochs, especially around the 1635 Å range.

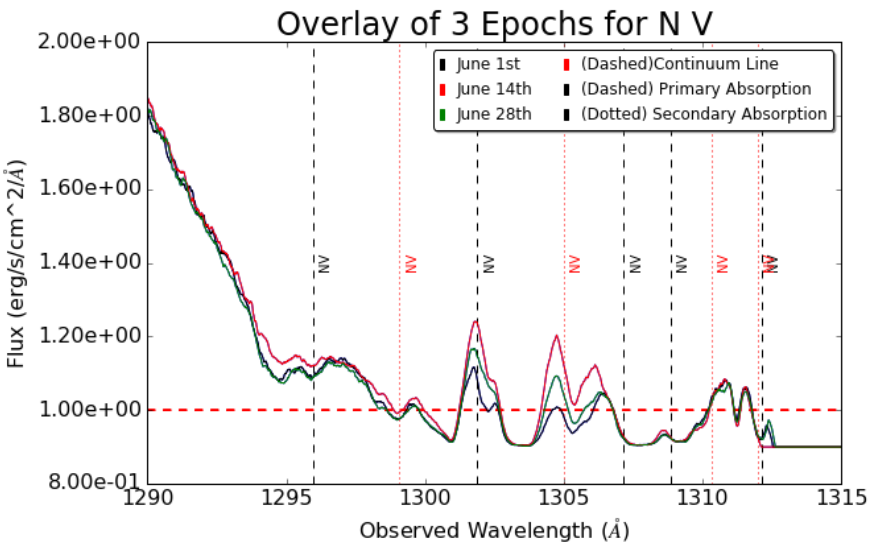

Figure 6: Overlay of all three epoch observations for Nitrogen V BALs. Here, the differences in the level of absorption is clearly present between the three epochs. For almost this entire plotted range, the level of absorption in epoch two is lower than that of epochs one and three. (Note: due to gap in grating used, no data present beyond ~1313 Angstroms)

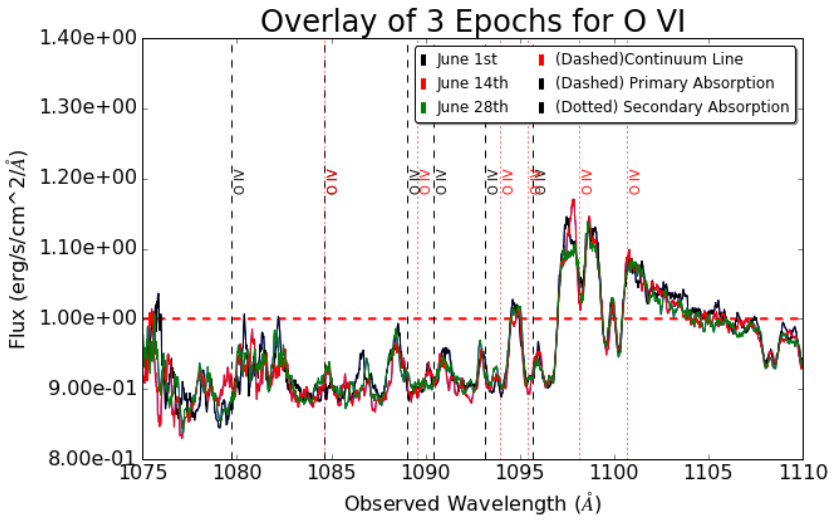

Figure 7: Overlay of all three epoch observations for Oxygen VI BALs. This region of the spectrum is difficult to investigate due to high "noise" levels.

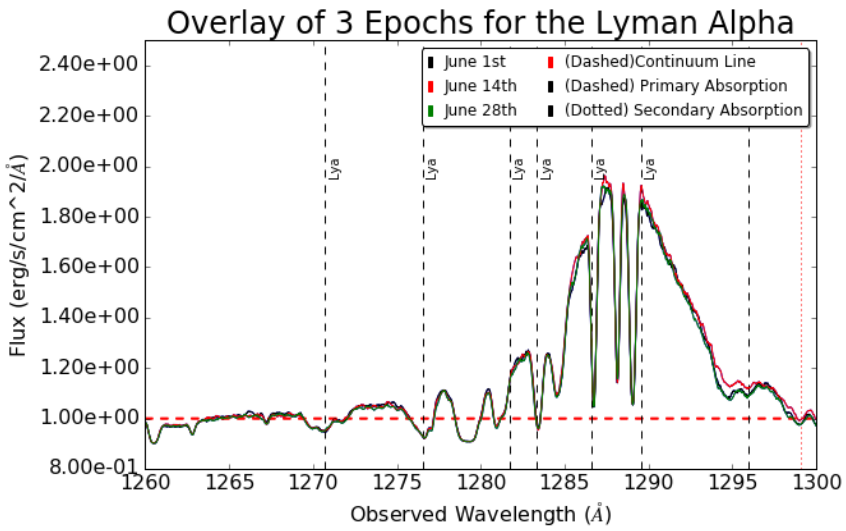

Figure 8: Overlay of all three epoch observations for Lyman-alpha BALs. Absorption is lower in the second epoch, most noticeably in the 1285 Å to 1290 Å range.

3. Results

3.1 Phosphorous V

At approximately 1186 Å is a BAL that disappears in the second epoch and reappears in the third. Another of these is possibly present at ~1177 Å. The flux level of the entire continuum is higher in the first epoch than the second and third epochs. The absorption region at ~1200 Å has the second epoch at a lower absorption level than the first and third epochs.

3.2 Silicon IV

The BALs at ~1466.5 Å and ~1476 Å are much shallower in the second epoch than in the first or third epochs.

3.3 Carbon IV

The BALs at 1621 Å, 1626 Å, 1635 Å, and 1637 Å are shallower in the second epoch than in the first or third. The red curve is visible above the black and green curves at the bottom of the BAL.

3.4 Nitrogen V

In the 1295 Å -1307 Å regions of the Nitrogen V spectra epoch 2 (red) has a higher flux than epoch 1 (black) and epoch 3 (green). By epoch 3 the level of absorption is closer to that of epoch 1 than epoch 2.

3.5 Oxygen VI

At approximately 1079 Å, the first and third epochs have values of zero flux, while the second epoch reaches ~0.35 erg/s/cm^2/ Å (before normalization and re-scaling). The amount of noise in this range of the spectrum makes it difficult to obtain knowledge of the absorption levels. A more accurate sensor may help clarify this part of the spectrum in the future.

3.6 Lyman-Alpha

When looking closely at the comparison between the three epochs, the levels of absorption at approximately 1287 Å and 1289 Å were lower in the second epoch than in the first and third epochs. The narrowness of the absorption lines in this region of the spectrum make it difficult to visually compare absorption levels.

4. Conclusions

These results show that the X-ray and UV absorption lines tend to be variable together. In the case of the X-ray portion of the spectrum, absorption levels had not returned to levels of the first epoch by the third epoch (reasoning for this phenomenon is beyond the scope of this paper). This tended to be the case in the observations, with some exceptions. For example, one of the exceptions was the absorption level of NV at approximately the 1297 Å range. Absorption was lower in the third epoch than in the first, and had not returned to the same relative levels of absorption of the 1300 Å- 1310 Å range. Observations of the OVI section of the spectrum (Figure 7) were not very useful in determining a pattern in absorption variability. This raises questions as to why most of the other UV spectrum measurements tended to follow the pattern of the X-ray epoch measurements while the OVI section did not.

5. Acknowledgments

This project was made possible by funding from the College of Natural Resources and Sciences of Humboldt State University, the guidance of Dr. Paola Rodriguez Hidalgo, the work of the NCUR editorial staff, as well as the programming knowledge from Dr. Ryan Campbell, stockroom technician Tyler Hooker, and fellow student Sean Haas.

6. References

1. Peterson B., “The central black hole and relationships with the host galaxy,” New Astronomy Reviews 52, (2008): 240-252

2. Sloan Digital Sky Survey, “First Discoveries”, http://skyserver.sdss.org/dr9/en/sdss/discoveries/discoveries.asp

3. Giustini M., Cappi M., Chartas G., Dadina M., Eracleous M., Ponti G., Proga D., Tombesi F., Vignali C., Palumbo G.G.C., “Variable X-ray absorption in the mini-BAL QSO PG 1126-041”, Astronomy & Astrophysics 536, (2011): A49

4. Narayanan D., Hamann F., Barlow T., Burbidge E. M., Cohen R. D., Junkkarinen V., Lyons R., “Variability of Narrow, Associated Absorption Lines in Moderate- and Low-Redshift Quasars,” APJ 613 (2004): 129-150

5. Rodriguez Hidalgo P., Hamann F., Hall P., “The extremely high velocity outflow in quasar PG0935+417,” MNRS 411, (2011): 247-259

6. Blandford R., “Active Galaxies and Quasistellar objects, Accretion”, NASA/IPAC Extragalactic Database, retrieved 5/18/16, http://ned.ipac.caltech.edu/level5/ESSAYS/Blandford/blandford.html